# THE ORBITAL PERIOD AND TIME-VARIABLE ASYMMETRIC ACCRETION DISK IN THE X-RAY BINARY MS 1603.6+2600 (=UW CORONAE BOREALIS)

PAUL A. MASON

Department of Physics, University of Texas at El Paso, El Paso, TX 79968; and Department of Mathematics and Physical Sciences,
New Mexico State University–Doña Ana, Las Cruces, NM 88003; pmason@nmsu.edu

EDWARD L. ROBINSON AND CANDACE L. GRAY

Department of Astronomy, University of Texas at Austin, 1 University Station C1400, Austin, TX 78712

AND

ROBERT I. HYNES

Department of Physics and Astronomy, Louisiana State University, Baton Rouge, LA 70803

## ABSTRACT

We present CCD photometry of the low-mass X-ray binary UW Coronae Borealis (UW CrB). Its light curve shows eclipses at a period near 111 minutes, but the eclipses vary in depth and shape and often disappear. Restricting our analysis to the deeper eclipses, we find the orbital period to be $110.976722 \pm 0.000012$ minutes, but the times of mideclipse can deviate by more than 0.025 in phase from the best-fit ephemeris. There is an additional large-amplitude variation with a period of $112.58 \pm 0.03$ minutes reminiscent of the superhumps seen in the light curves of some cataclysmic variables. The variations of the eclipse morphology are not random, repeating at a period near 5.5 days, and the shape of the superhump-like modulation also varies at this period. We interpret the light curve as the eclipse of the accretion disk around the neutron star by the secondary star. The surface brightness of the accretion disk is strongly asymmetric and highly variable, producing the variations of the eclipse morphology and times of mid-eclipse. A model in which the distribution of surface brightness is elliptical and precesses at the 5.5 day period re-produces the eclipse depths and the times of mideclipse reasonably well. As 112.6 minutes is the beat period between 110.97672 minutes and 5.5 days, the superhump-like variability is closely related to the precessing elliptical disk, but the causal relationship is unclear.

*Subject headings:* accretion, accretion disks — binaries: close — binaries: eclipsing — stars: individual (MS 1603.6+2600, UW CrB) — X-rays: binaries

## 1. INTRODUCTION

The interacting binary UW CrB is the optical counterpart of the X-ray source MS 1603.6+2600 (Gioia et al. 1990). The first detailed study of UW CrB was by Morris et al. (1990), who found eclipses up to ~0.7 mag deep in its light curve and used them to determine an orbital period of $111.04 \pm 0.04$ minutes. From its X-ray emission, short orbital period, and emission-line spectrum, they concluded that UW CrB is either a cataclysmic variable or a low-mass X-ray binary (LMXB). The ratio of its X-ray–to–optical fluxes $F_X/F_{opt}$ is unusual, ~10 times higher than most cataclysmic variables but much lower than most LMXBs. The eclipse profile is highly variable, the eclipses often disappear, and the light curve shows other rapid variations with amplitudes up to ~0.5 mag, making period finding difficult. Thus Vilhu et al. (1993) could not confirm the 111 minute period but did find a period at 112.5 minutes; and Hakala et al. (1998) were unable to find any definite period at all. Ergma & Vilhu (1993) discussed three possible LMXB evo-lutionary models that could reproduce the properties of UW CrB, but did not eliminate cataclysmic variable models.

Mukai et al. (2001) obtained *ASCA* data showing an X-ray flare that they interpreted as a type I X-ray burst. Since a type I burst would require that the accreting object be a neutron star, Mukai et al. (2001) suggested that UW CrB is a dipping LMXB at a dis-tance of about 75 kpc. Jonker et al. (2003) noted that if UW CrB is at 75 kpc, its optical luminosity would be far larger than that of any other dipping source, and argued instead that UW CrB is an accretion disk corona (ADC) source. Because ADC sources are

viewed from near the orbital plane, their neutron stars are obscured by the accretion disk, reducing the observed X-ray flux. Inter-preting UW CrB as an ADC source reduces its inferred distance and explains its low $F_X/F_{opt}$. Hynes et al. (2004) and Muhli et al. (2004) discovered multiple optical bursts from UW CrB, which they identified as reprocessed type I X-ray bursts, and Hakala et al. (2005) discovered additional multiple X-ray bursts, confirming that the accreting star is a neutron star. All these authors favor the ADC model and a distance less than 10 kpc.

The X-ray light curve of UW CrB has been measured by Hakala et al. (1998) with the PSPC on *ROSAT*, by Mukai et al. (2001) with *ASCA*, by Jonker et al. (2003) with the *Chandra X-Ray Observatory*, and by Hakala et al. (2005) with *XMM-Newton*. Strikingly, the eclipse that is so prominent at optical wavelengths is completely absent at energies greater than 2 keV. Some of the soft X-ray (<2 keV) light curves showed dips that might or might not be eclipses, but if they are, the eclipses are shallow, noisy, and often entirely missing. All the X-ray light curves show a large-amplitude modulation at roughly the orbital period. While the mod-ulation is present at all wavelengths, its amplitude is much larger in the 0.1–1.0 keV band than at higher energies. The shape of the modulation varies from epoch to epoch. Because of the lack of repeating eclipses and because the modulation is strongest at low energy, Hakala et al. (2005) attribute the modulation to variable absorption by the rim of the accretion disk, perhaps because the rim height varies around the disk.

While it is now clear that the compact star in UW CrB is a neu-tron star and that the optical eclipses are eclipses of an accretion

disk around the neutron star, many basic properties of the system remain unknown. In particular, the orbital period, the origin of the large-amplitude variability at optical wavelengths, and the geometry of the accreting material are all uncertain. In this paper we present new optical photometry of UW CrB. Combining our photometry with previously published photometry we show that the orbital period is 110.97672 minutes, but also that the times of mideclipse deviate systematically from the times predicted by the eclipse ephemeris. The large-amplitude variations have properties reminiscent of the superhumps seen in the light curves of some cataclysmic variables. We show that the changes in the morphologies of the eclipse and of the superhump-like variations are not random, but repeat at a period near 5.5 days, leading to a 112.6 minute beat period. Finally we show that a model in which the surface brightness of the accretion disk has a roughly elliptical distribution that precesses with a 5.5 day period reproduces the eclipse profiles, the times of mideclipse, and the nearly constant mean optical luminosity reasonably well.

## 2. THE PHOTOMETRIC DATA

We obtained new CCD photometry of UW CrB with the McDonald Observatory 2.7 m telescope on 20 nights in 2002, 2003, and 2004. Observations were made through $B$, $V$, and $R$ filters, although most of the data were obtained using just the $R$ filter to sample the light curves more frequently. The $R$-band integrations were typically 1 minute long. Much of the data were obtained through thin clouds, but the field of UW CrB contains enough comparison stars to allow good photometry, even under mediocre sky conditions. The raw CCD images were reduced using standard IRAF routines, and the aperture photometry was performed using a combination of IRAF routines and a custom IDL script. The times of the data points were individually converted to Heliocentric Julian Date (HJD). Further information about the observing runs is given in Table 1, and examples of the resulting light curves are shown in Figures 5 and 6.

To this new data set we added the already existing high-speed photometry described in Hynes et al. (2004). The high-speed photometry was obtained in 2004 on the 2.1 m telescope at McDonald Observatory with the Argos photometer through a broadband $BVR$ filter at sampling intervals of 5 or 10 s. We also added the photometry of UW CrB published by Morris et al. (1990) and Hakala et al. (1998). We extracted this photometry from magnified versions of the figures in the papers showing the light curves, measuring the individual points in the figures. To check the extracted photometry we reanalyzed it, finding periods identical to those reported by the original investigators. All this photometry was obtained in white light (unfiltered CCD detectors), with the exception of three nights of $V$-band data from Hakala et al. (1998). Both the new and previously published photometry are differential relative to the same comparison star, star "V" in Figure 1 of Hakala et al. (1998). There are systematic offsets between the light curves, which we attribute primarily to the different photometric bandpasses used to measure the various light curves. In all we have photometry from 40 nights between 1989 and 2004.

## 3. THE ORBITAL PERIOD

The reason why the orbital period of UW CrB has been so difficult to measure is that the morphology of the light curve is highly variable. While many eclipses are deep and easily identifiable, many are so shallow that they are masked by the other large-amplitude variations in the light curve; and conversely the other variations can mimic shallow eclipses. The light curves shown in Figure 1 of Hynes et al. (2004) nicely exemplify this behavior. We will also see that the times of mideclipse deviate from the times

TABLE 1
JOURNAL OF OBSERVATIONS

| UT Date (UT) | Start Time (HJD −2,450,000.0) | Length (hr) | Data Points |
|---|---|---|---|
| 2002 Jun 09 .......... | 2434.64012 | 2.45 | 207 |
| 2002 Jun 10 .......... | 2435.64084 | 0.87 | 46 |
| 2002 Jun 12 .......... | 2437.65202 | 0.07 | 6 |
| 2002 Jun 14 .......... | 2439.63679 | 4.20 | 260 |
| 2002 Jul 12 .......... | 2467.64015 | 2.41 | 108 |
| 2002 Jul 13 .......... | 2468.64529 | 2.99 | 126 |
| 2002 Jul 14 .......... | 2469.64970 | 2.76 | 99 |
| 2002 Jul 15 .......... | 2470.73493 | 0.87 | 42 |
| 2003 Jun 29 .......... | 2819.73094 | 1.92 | 79 |
| 2003 Jun 30 .......... | 2820.63841 | 2.79 | 77 |
| 2003 Jul 01 ........... | 2821.63883 | 1.57 | 79 |
| 2003 Jul 02 ........... | 2822.63732 | 1.64 | 79 |
| 2003 Jul 03 ........... | 2823.63812 | 1.73 | 79 |
| 2004 Apr 16.......... | 3111.84007 | 3.64 | 1313 |
| 2004 Apr 18.......... | 3113.93078 | 1.23 | 445 |
| 2004 Apr 21.......... | 3116.83794 | 3.61 | 1302 |
| 2004 Apr 22.......... | 3117.82275 | 3.79 | 2728 |
| 2004 Apr 23.......... | 3118.74217 | 5.80 | 4191 |
| 2004 May 12......... | 3137.67470 | 5.77 | 192 |
| 2004 May 13......... | 3138.66416 | 6.73 | 294 |
| 2004 May 14......... | 3139.67176 | 4.38 | 208 |
| 2004 May 15......... | 3140.69302 | 2.10 | 71 |
| 2004 May 17......... | 3142.80184 | 3.55 | 175 |
| 2004 Jun 15 .......... | 3171.66696 | 5.61 | 265 |
| 2004 Jun 21 .......... | 3177.63714 | 1.41 | 60 |

predicted by a strictly periodic ephemeris. Finally, the light curves of compact binaries are often multiperiodic, and some periods, especially superhump periods (Patterson 2001), are easily confused with the orbital period.

To overcome these difficulties, we determined the orbital period in two different ways. First we used a simple and unbiased periodogram technique with the intent of overwhelming the problem with our large mass of data. Considering the obvious complexity of the light curve, this method requires caution and is best employed with other techniques. Second, we used the traditional technique of measuring the times and cycle counts of the eclipses and then refining the period with an $(O - C)$ diagram, but restricting the data set to the deepest and most prominent eclipses. Both techniques yielded a unique and well-determined period, and the periods from the two techniques agree.

For the periodogram we used the phase dispersion minimization (PDM) technique (Stellingwerf 1978). This method calculates a periodogram by (1) phasing all the data at a chosen period, (2) dividing the data into phase bins and determining the standard deviation of the data within each bin, (3) summing the standard deviations from all the bins to form the phase dispersion statistic, and (4) repeating the process across the appropriate range of periods. The phase dispersion is lower at periods where there are strong periodic signals. The PDM technique is useful when large amounts of data are available, and the periodic signal has much power in the higher harmonics of the fundamental period. Before calculating the periodogram the high-speed photometry from Hynes et al. (2004) was binned to a resolution of 15 or 20 s so that it was not overweighted in the analysis; and scale factors were applied to remove the offsets caused by the different photometer bandpasses.

The relevant portion of the PDM periodogram for UW CrB is shown in Figure 1. There is a well-defined minimum at $110.97672 \pm 0.00002$ minutes with symmetrical sidelobes corresponding to 1 and 2 yr aliases. There are no other comparably deep minima in
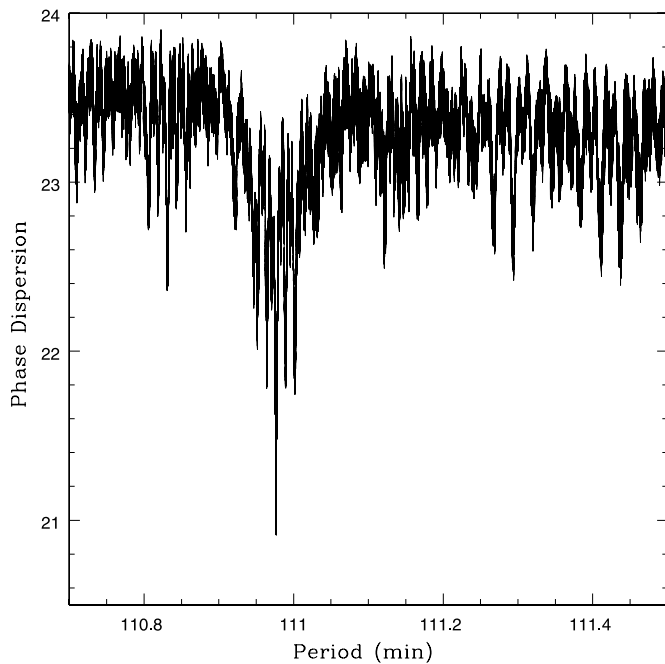
Fig. 1.—Portion of the phase dispersion periodogram for the light curve of UW CrB. The deepest minimum is at ∼110.97672 ± 0.00002 minutes. The nearby minima are sidelobes corresponding to 1 and 2 yr aliases. There are no other comparably deep minima in the periodogram.

TABLE 2
TIMES OF MIDECLIPSE

| Eclipse Number | Mideclipse Time (HJD −2,400,000.0) | Uncertainty (days) |
|---|---|---|
| −70692 | 47,670.8031 | 0.0014 |
| −70691 | 47,670.8817 | 0.0014 |
| −70690 | 47,670.9582 | 0.0014 |
| −70680 | 47,671.7297 | 0.0014 |
| −70679 | 47,671.8078 | 0.0014 |
| −70667 | 47,672.7313 | 0.0014[a] |
| −70666 | 47,672.8101 | 0.0014 |
| −70664 | 47,672.9637 | 0.0014[a] |
| −70654 | 47,673.7336 | 0.0014[a] |
| −70653 | 47,673.8114 | 0.0014[a] |
| −61442 | 48,383.6740 | 0.0014 |
| −60702 | 48,440.7040 | 0.0014 |
| −60701 | 48,440.7820 | 0.0014 |
| −60700 | 48,440.8570 | 0.0014 |
| −8449 | 52,467.6955 | 0.0011 |
| −3856 | 52,821.6680 | 0.0011 |
| −25 | 53,116.9120 | 0.0007 |
| −13 | 53,117.8350 | 0.0007 |
| −12 | 53,117.9115 | 0.0007 |
| −1 | 53,118.7590 | 0.0007 |
| 0 | 53,118.8365 | 0.0007 |
| 1 | 53,118.9140 | 0.0007 |
| 271 | 53,139.7215 | 0.0011 |
| 272 | 53,139.7980 | 0.0011 |

[a] Eclipse times that were not used in the original period determination.

the periodogram. Vilhu et al. (1993) found a period of 112.5 minutes in their data, not 111 minutes, and our periodogram also shows a shallow minimum near 112.6 minutes. By accident the Vilhu et al. (1993) data set had very few eclipses. As we will show in the next section, when we remove the deepest eclipses from our data set, the 110.97672 minute period is weakened and the 112.6 minute period becomes the second strongest signal in the periodogram. This implies that the 110.97672 minute period refers to the eclipse period and, thus, to the orbital period. The 112.6 minute period refers to the other large-amplitude variations.

To find the orbital period from the times of eclipses we first selected the deepest and most prominent eclipses. Using only deep eclipses avoids inclusion of spurious eclipses caused by other variations in the light curves, and it avoids the use of real but shallow eclipses for which the measured times may have large errors. There are 20 well-sampled eclipses deeper than ∼0.4 mag in our data set; their times of mideclipse are listed in Table 2. We determined the cycle counts for the eclipses in two ways. The first was by "bootstrapping" the cycle counts and orbital period in the usual way from eclipses separated by short intervals of time to eclipses separated by longer intervals. Because of concerns that the times of minima might be strongly affected by rather small variations in the shape of the eclipse minima, we also developed a computer program that uses the entire eclipse light curve. This is an interactive program that allows the user to choose a subset of the light curves, fold the light curves at a given period, and display the superimposed folded light curves. The user can easily tune the period to the one that yields the least apparent scatter in the superimposed eclipse light curves. Measurement of the cycle counts and the orbital period then proceeds in the same way as using times of mideclipse. The light-curve comparison method provides a high degree of confidence in the determination of the best period and the range of allowable periods.

Although the data have the usual gaps at 1 month and 1 yr intervals, and a large gap from 1992 to 2001, there is much redundancy in the eclipse timings, allowing the cycle counts and orbital

period to be determined uniquely. In fact, the interactive program appears to discriminate against aliases more strongly than the periodogram technique, perhaps because light curves with weak or spurious eclipses do not degrade the period determination. The cycle counts for the eclipses are given in Table 2. Armed with reliable cycle counts, we calculated the best-fit ephemeris for the times of mideclipse by least squares. For this final calculation we included four additional times of mideclipse listed by Morris et al. (1990), two of which did not satisfy our criteria for strong eclipses, and two were measured from spectrophotometry. The best-fit linear ephemeris for the 24 times of mideclipse is

$$T_{\mathrm{mid}} = \mathrm{HJD}\ 2{,}453{,}118.8367(4) + 0.077067168(8)E, \quad (1)$$

where $E$ is the eclipse number. The corresponding orbital period is 110.976722 ± 0.000012 minutes, the same as the period determined from the periodogram. The $(O - C)$ diagram for the linear ephemeris is shown in Figure 2.

We also fit a quadratic ephemeris to the eclipse times, finding

$$T_{\mathrm{min}} = \mathrm{HJD}\ 2{,}453{,}118.8367(4) + 0.077067357(68)E$$
$$+ 2.7(1.0) \times 10^{-12}E^2. \quad (2)$$

The reduced $\chi^2$ for the linear fit is 1.64, while that of the quadratic fit is 1.56. The improvement is not statistically significant, so the data do not currently require a quadratic ephemeris nor the changing orbital period it would imply.

The reduced $\chi^2$ for both the linear and quadratic ephemerides are significantly greater than 1.0, demonstrating that the eclipse times scatter about the times predicted by the ephemerides by more than the measurement error. Figure 3 shows two eclipses with large residuals in the $(O - C)$ diagram. The residuals can be up to ∼0.025 in orbital phase for the deeper eclipses. The residuals are larger for the shallower eclipses, but some or all of the increased
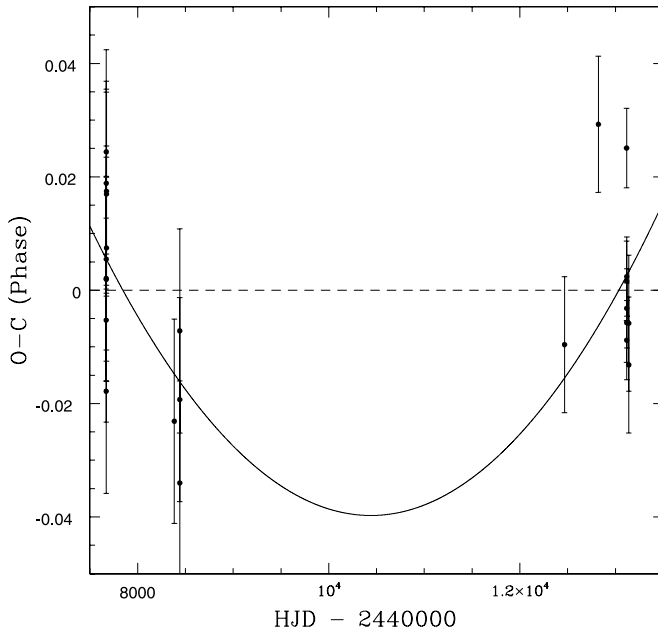
FIG. 2.—The $(O - C)$ diagram for the times of eclipses; $O$ is the observed time of mideclipse, and $C$ is the time predicted from the linear ephemeris of eq. (1). Observed times that agree with the calculated times would fall on the horizontal dashed line. The curved solid line is the quadratic ephemeris of eq. (2). The $\chi^2$ for the quadratic ephemeris is smaller than the $\chi^2$ for the linear ephemeris, but the improvement is not statistically significant.

residuals may be caused by the greater measurement error for the shallower, noisier eclipses. Figure 3 also shows that eclipses with large residuals can be both wide and relatively symmetric.

## 4. OTHER PHOTOMETRIC VARIATIONS

The light curve of UW CrB varies by up to ∼0.5 mag outside of the eclipses. At first glance the variations are random and, indeed, the PDM periodogram of our entire data set shows no significant minima at periods other than the orbital period. If, however, the portions of the light curves containing deep eclipses are removed from the data set, the PDM periodogram (Fig. 4) shows a broad minimum at $P_{hump} = 112.58 \pm 0.03$ minutes, essentially
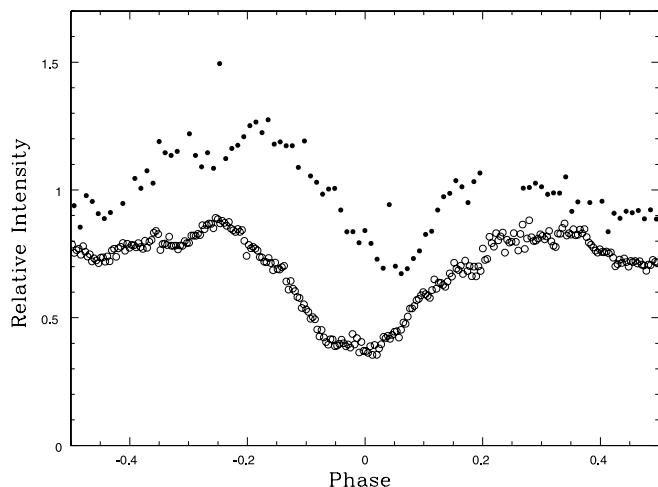


FIG. 3.—*Filled circles*: Eclipse light curve from 2004 May 17. *Open circles*: Eclipse light curve from 2004 April 23. The orbital phase is calculated from the linear ephemeris of eq. (1). The times of eclipse are displaced from phase 0, illustrating the deviations in times of mideclipse that produce the large $\chi^2$ for the ephemeris. The light curve from 2004 April 23 shows that eclipses with large displacements can be both wide and relatively symmetric.
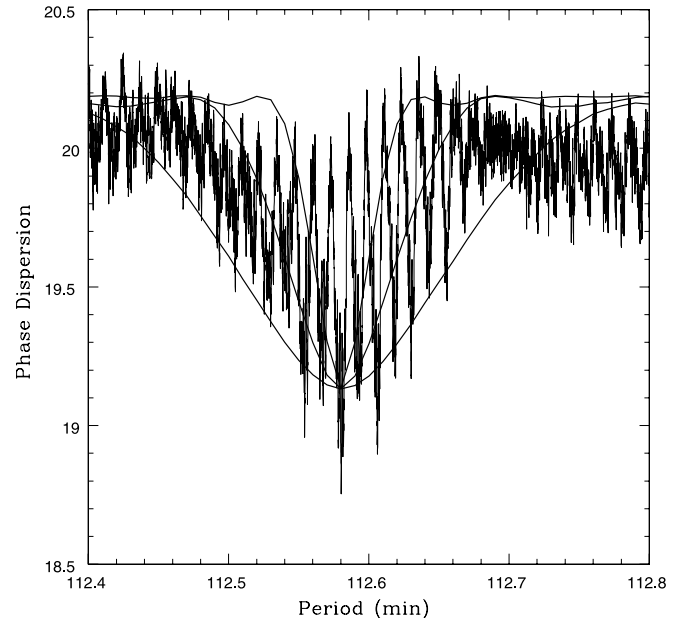


FIG. 4.—Portion of the phase dispersion periodogram for the light curve of UW CrB with deep eclipses excised, shown along with three smooth periodograms to demonstrate phase coherence. There is a broad minimum at 112.58 ± 0.03 minutes, although it is chopped up by a myriad of narrow minima due to yearly aliases. This minimum is substantially broader than the minimum at the 110.97672 minute orbital period (see Fig. 1), from which we infer that the 112.58 minute modulation is not strictly periodic. The three smooth curves are periodograms of sine waves, including noise, with periods of 112.58 minutes sampled over baselines of 40, 80, and 160 days; with the narrowest being from 160 days. This indicates a coherence timescale of ∼80 days for this secondary period.

the same period found by Vilhu et al. (1993). While sharp minima due to yearly aliases chop up and obscure the periodogram, the minimum near 112.6 minutes is clearly much broader than the minimum at the 110.97672 minute orbital period. We infer that the 112.6 minute modulation is not strictly periodic. Coherence of this period can be estimated by direct comparison of the periodogram with that of strictly periodic data trains of various lengths. This analysis, shown in Figure 4, indicates that this periodicity maintains coherence for ∼80 days. Thus the 112.6 minute period maintains coherence over much of an observing season but not from year to year. For completeness we mention that the periodogram also shows an array of five broad, weak minima spaced at intervals of ∼(112.58 − 110.97672)/6 minutes between 110.97672 and 112.6 minutes. These are likely 1 month aliases.

The period excess of the 112.6 minute modulation is $\epsilon = (P_{hump} - P_{orb})/P_{orb} \approx 0.0145$, suggesting the modulation might be a superhump. According to superhump theory $\epsilon$ should be a function of the mass ratio (Mineshige et al. 1992; Warner 1995). If the mass of the neutron star in UW CrB is 1.35 $M_\odot$ and the mass of the secondary star is 0.2 $M_\odot$ (Thorsett & Chakrabarty 1999; Howell et al. 2001), the mass ratio of UW CrB is $q = M_2/M_{ns} \approx 0.15$. With this mass ratio UW CrB lies somewhat below the empirical $\epsilon(q)$ relation for cataclysmic variables but close to an extension of the relation for X-ray binaries (see O'Donoghue & Charles [1996] and Fig. 3 in Patterson [2001]). It also lies close to the theoretical relation given by Pearson (2006) for systems with a primary mass $M_1 = 1.44 \ M_\odot$, which is the appropriate relation for neutron star binaries. Thus the period excess supports a superhump interpretation for the 112.6 minute modulation.

On the other hand, Haswell et al. (2001) have argued convincingly that the superhump-like variations sometimes observed in the light curves of LMXBs and soft X-ray transients cannot be precisely the same phenomenon as the superhumps observed in
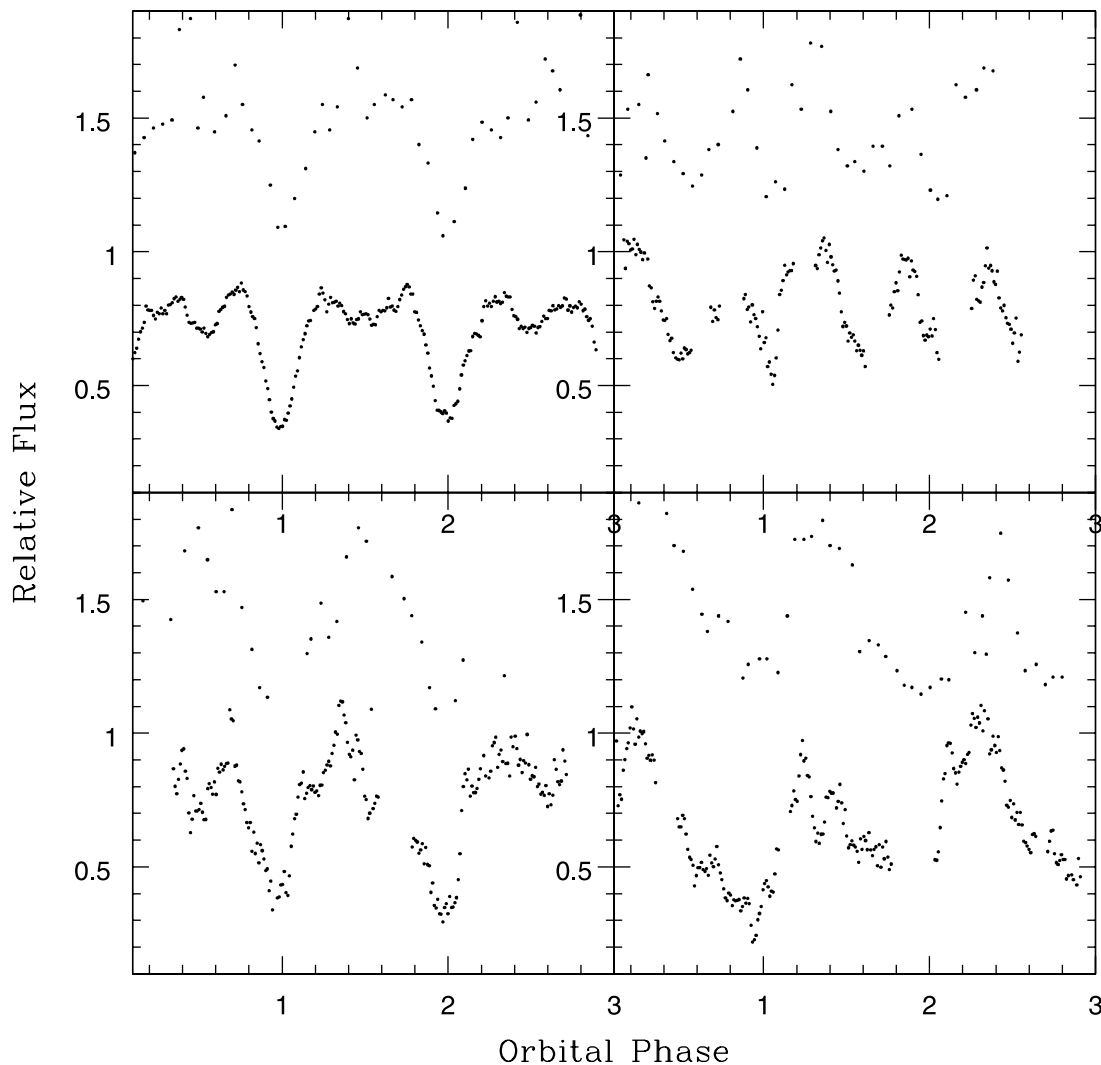
FIG. 5.—Four pairs of light curves with similar morphology, even though separated by more than a decade. Although the morphology of the light curve of UW CrB varies greatly from night to night, the variations are not random, but repeat at a 5.5 ± 0.1 day recurrence period. The light-curve pairs are (*top light curve, first; bottom, second*) as follows: *top left panel*: 1991 July 3, 2004 April 23; *top right panel*: 1991 July 24, 2004 May 13; *bottom left panel*: 1991 May 7, 2004 May 14; *bottom right panel*: 1991 July 2, 2004 May 13.

the light curves of cataclysmic variables. To reprise their argument: In cataclysmic variables with mass ratios less than ∼0.25, the accretion disk can become large enough to encompass the 3 : 1 resonance with the orbital period. If so, the disk becomes elliptical and begins to slowly precess ( Murray 2000). Superhumps in these systems are caused by tidally driven modulation of viscous dissipation in the outer parts of the elliptical disk. The superhump period is a few percent longer than the orbital period because of the slow disk precession. In LMXBs, however, the optical emission from the disk comes from reprocessing of X-rays originating near the center of the disk. The reprocessed energy swamps the energy produced in the outer disk by viscous dissipation, so the mechanism producing the superhump variations in cataclysmic variables is ineffective for LMXBs. We will show in the next section that the 112.6 minute modulation is, nevertheless, closely related to true superhumps, even though the specific emission mechanism producing the modulation cannot be the same as in the cataclysmic variables. Therefore we refer to the variations as a "superhump-like" modulation.

The morphology of the superhump-like modulation varies from night to night, and the eclipse depth also varies from night to night. The two variations are strongly correlated, leading to light-curve

shapes that recur. Figure 5 shows four pairs of similar light curves separated by more than a decade, selected to show a range of eclipse depths. When the eclipses are deepest, the superhump-like variations have a lower amplitude and tend to be symmetric about the eclipse. As the eclipse grows shallower, the amplitude of the superhump-like variations increases and they become more asymmetric. The similar light curves recur periodically or at least quasi-periodically. The light curves displayed in Figure 1 of Hynes et al. (2004) show that the recurrence time must be longer than about 4 days. Our data set has enough pairs of recurrent light curves to limit the recurrence period to $P_{recur} = 5.5 \pm 0.1$ days. This period is strictly determined only for the 2004 observing season. Hakala et al. (2005) mention in passing that they too find a ∼5 day period in unpublished optical data, so the 5.5 day period is a real property of UW CrB, not just a statistical fluke.

The 5.5 day period yields a consistent ordering of the light-curve morphologies. Figure 6 shows light curves of UW CrB ordered by phase within the 5.5 day period, where phase 0 of the 5.5 day period is defined to be the time when the eclipse has its maximum depth. As the phase increases from 0, the eclipse becomes progressively shallower, nearly disappearing at phase 0.5, and then becoming progressively stronger again. Figure 6 also
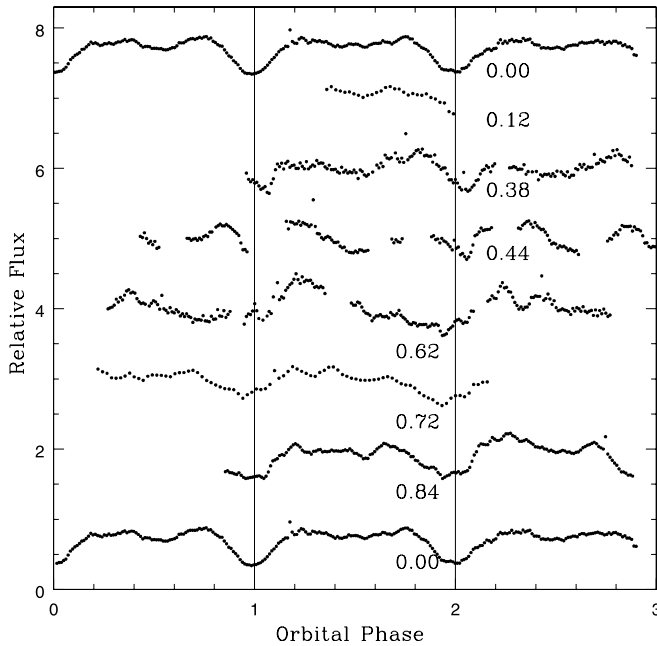
Fig. 6.—Light curves of UW CrB arranged in order of phase in the 5.5 day period. The light curves come from days ( *from top to bottom*) 2004 April 23, 2004 April 18, 2004 May 17, 2004 May 12, 2004 May 13, 2004 April 16, 2004 April 22, and 2004 April 23 again. Phase 0 of the 5.5 day period is defined to be when the deepest eclipses occur. As the phase increases from 0, the eclipse becomes progressively shallower, nearly disappearing near phase 0.5; then after phase 0.5 becoming progressively deeper again. The times of eclipse can be advanced or delayed by 0.03 or more in orbital phase.

reveals a pattern to the deviations in the times of mideclipse. At phase 0 in the 5.5 day period the eclipse occurs close to the time given by the orbital ephemeris, but before phase 0 the eclipse occurs systematically early, and after phase 0 the eclipse occurs systematically late. Near phase 0 the superhump-like modulation has a low-amplitude, little rapid variability, a double peak, and is symmetric about the eclipse. Near phase 0.5 the modulation has a larger amplitude, much rapid variability, and a single asymmetric peak.

The beat period between the 5.5 day period and the orbital period is equal to the period of the superhump-like modulation:

$$\left( \frac{1}{P_{\rm orb}} - \frac{1}{P_{\rm recur}} \right)^{-1} = 112.55 \pm 0.03 \text{ minutes} \approx P_{\rm hump}. \quad (3)$$

This beat relation and the covariation of the eclipse properties with the superhump-like modulation at the 5.5 day period show that the eclipse variations are closely related to the superhump-like modulation.

## 5. AN ELLIPTICAL, PRECESSING ACCRETION DISK

The optical light curves of UW CrB show eclipses whose depths vary from less than a few tenths of a magnitude to ∼0.6 mag with relatively little concomitant change in the mean flux at orbital phases outside eclipse. The homogeneous data sets in Hakala et al. (1998) and Hynes et al. (2004) display this behavior well. The variable eclipse depth shows that the projected geometry of the disk changes greatly, but the nearly constant mean flux outside eclipse shows that the projected surface area of the accretion disk remains roughly constant. These two conditions impose strong constraints on models for the disk geometry. They eliminate, for example, circular disks with variable radius and precessing disks twisted out of the orbital plane (e.g., Haswell et al. 2001; Foulkes et al. 2006).

A circularly symmetric disk with variable radius also cannot account for the systematic deviations in the times of eclipse minimum.

A surprisingly simple model does account for the eclipses and their variations. The only source of light in the model is a flat disk lying in the orbital plane. The disk has a nonzero surface brightness only inside an elliptical region with the neutron star at one focus of the ellipse, and the ellipse precesses with a period of 5.5 days. Two points should be noted. First, we do not imagine that the distribution of surface brightness is truly elliptical; an ellipse is merely a low-order approximation to the true distribution. Second, eclipses reveal the distribution of emitted flux, not the distribution of mass. We will see that a highly eccentric distribution of surface brightness is required to match the eclipses of UW CrB; the distribution of mass may be less eccentric.

The mass ratio $q$ and orbital inclination $i$ are needed to calculate the eclipse light curves. Following the discussion in the previous section we adopt $q = 0.15$. Once the mass ratio has been specified, the orbital inclination is tightly constrained. For any model in which a significant amount of flux comes from near the center of the disk, deep eclipses are possible only if the orbital inclination is high enough that most of the central disk is eclipsed. This limits the orbital inclination to $i \gtrsim 77°$. Conversely, it is impossible to produce shallow eclipses if most of the disk is eclipsed. Even for a disk so large that its outer edge approaches the tidal truncation radius at ∼0.45$a$ (Frank et al. 2002), where $a$ is the separation of the two stars, the disk is eclipsed all the way to its back edge if $i \gtrsim 81°$. The orbital inclination is, therefore, constrained to lie in the range $77° \lesssim i \lesssim 81°$. The salient property of the X-ray light curve of UW CrB is the lack of eclipses. If X-rays from the neutron star were directly visible, the lack of eclipses would limit the orbital inclination to less than $77.5°$. However, if the ADC model for UW CrB is correct, the neutron star is obscured by an optically thick ADC or a vertically extended inner disk, so most of the observed X-ray flux comes from above the orbital plane. This increases the upper limit on the orbital inclination by a few degrees. We adopt $i = 79°$. While this precise choice for $i$ depends on the adopted value of $q$—which is based on theoretical, not observational, considerations—other choices of $q$ and $i$ yield qualitatively similar results and do not change our conclusions.

Given $q$ and $i$ the only free parameters in the model are the semimajor axis $a_{\rm disk}$, eccentricity $e$, and distribution of surface brightness distribution across the ellipse. These can be adjusted to produce eclipses that match the observed eclipse widths, the range of eclipse depths, and jitter of the eclipse times. Figure 7 shows eclipse light curves for ellipses with a uniform surface brightness, each panel corresponding to a specific combination of $a_{\rm disk}$ and $e$. The deepest eclipse in each panel occurs when the long end of the disk major axis points at the secondary star, and the shallowest occurs when the major axis points away from the secondary. The two eclipses of intermediate depth correspond to the major axis pointing $60°$ to one side or the other of the line joining the centers of the stars, which is close to the time of maximum displacement $\Delta\phi_{\rm max}$ of the eclipses from orbital phase 0. The top panel shows eclipses for $a_{\rm disk} = 0.3a$ and $e = 0.5$, for which the maximum and minimum distances of the disk edge from the neutron star are $0.3a(1 \pm e)$, or 0.45$a$ and 0.15$a$. This combination yields $\Delta\phi_{\rm max} = \pm 0.028$. For the middle panel $a_{\rm disk} = 0.3a$ and $e = 0.25$, yielding $\Delta\phi_{\rm max} = \pm 0.013$; and for the bottom panel $a_{\rm disk} = 0.15a$ and $e = 0.5$, yielding $\Delta\phi_{\rm max} = \pm 0.011$. The amount of jitter, the eclipse widths, and the range of eclipse depths all increase as $a_{\rm disk}$ and $e$ increase. The light curves in the top panel, with $a_{\rm disk} = 0.3a$ and $e = 0.5$, roughly reproduce the observed eclipse widths, depths, and jitter. The model is too primitive and, as we will show below, too incomplete to justify a quantitative fit to the data, but
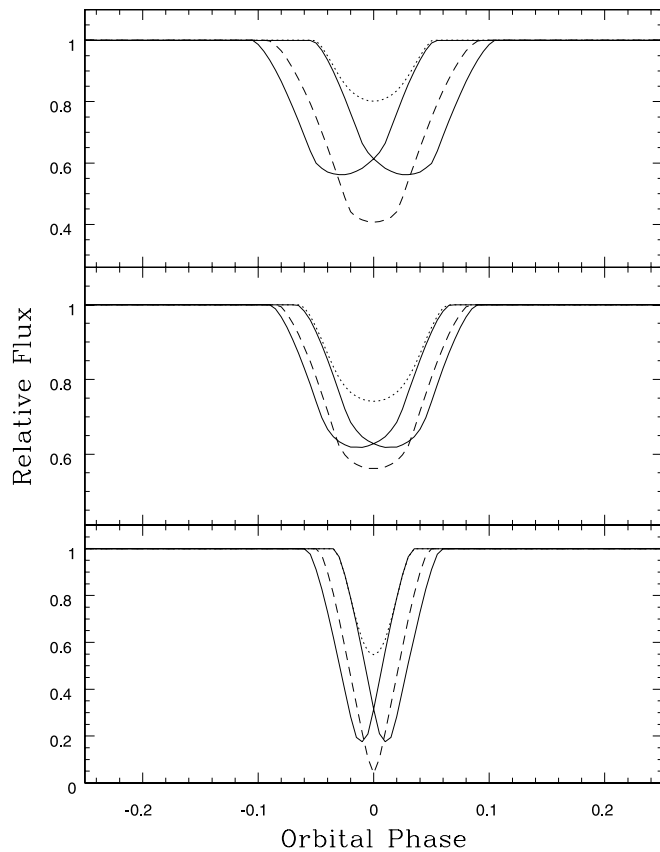
Fig. 7.—*Each panel*: Four eclipses of a disk with an elliptical distribution of surface brightness. The surface brightness of the disk is uniform within the ellipse and zero outside the ellipse. In each panel the deepest eclipse occurs when the long end of the disk major axis points at the secondary star, and the shallowest occurs when the major axis points away from the secondary. The two eclipses of intermediate depth correspond to the major axis pointing $60°$ to one side or the other of the line joining the centers of the stars, which is close to the time of maximum displacement $\Delta\phi_{max}$ of the eclipses from orbital phase 0. The three panels differ by the geometry of the ellipse, specified by the disk semimajor axis $a_{disk}$ and eccentricity $e$, and the resulting displacement. The top panel is the closest fit to the eclipses of UW CrB. *Top*: $a_{disk} = 0.3a$, $e = 0.5$, yielding $\Delta\phi_{max} = \pm 0.028$. *Middle*: $a_{disk} = 0.3a$, $e = 0.25$, yielding $\Delta\phi_{max} = \pm 0.013$. *Bottom*: $a_{disk} = 0.15a$, $e = 0.5$, yielding $\Delta\phi_{max} = \pm 0.011$.

it is clear that both $a_{disk}$ and $e$ must be large to reproduce the observed eclipses. To match the observed sign of the jitter, the disk must be precessing in the prograde direction.

Figure 8 shows the effect of nonuniform surface brightness on the eclipses. All the light curves in the figure show eclipses of a disk with a nonzero surface brightness only inside an elliptical region with $a_{disk} = 0.3a$ and $e = 0.5$ (the same as for the upper panel of Fig. 7); and for all the light curves the elliptical distribution points $60°$ to one side of the line joining the centers of the two stars. This configuration maximizes the effect of a nonuniform brightness distribution on the shape of the eclipse. The solid lines in both panels show an eclipse of an ellipse with a uniform surface brightness. In the upper panel the shallower dashed curve shows the eclipse of an ellipse with the $r^{-3/4}$ temperature distribution of a steady state, optically thick $\alpha$-model accretion disk. The deeper dashed curve shows the eclipse of an ellipse with a uniform surface brightness on which a bright spot has been superimposed near the outer edge. The spot covers the outer 1/3 of the disk radius, it extends $60°$ around the disk, and it has a surface brightness 4 times greater than the underlying disk. The eclipses are too asymmetric and too narrow to match the observed light curves. In the lower panel the dashed line is the eclipse of a disk
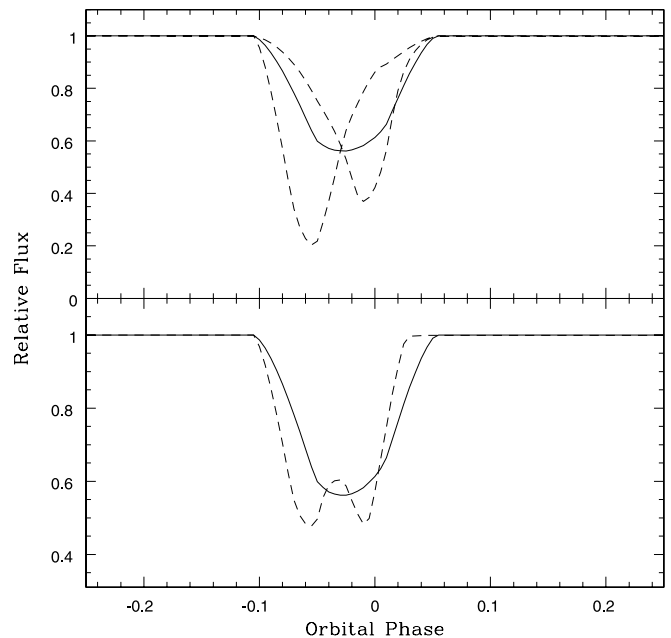


Fig. 8.—Effect of nonuniform surface brightness on the eclipses. All the light curves in both panels show eclipses of a disk with an elliptical distribution of light with $a_{disk} = 0.3a$ and $e = 0.5$; and for all the light curves the elliptical distribution points $60°$ to one side of the line joining the centers of the two stars. The solid line in both panels shows an eclipse of an ellipse with a uniform surface brightness. *Upper*: The shallower dashed curve shows the eclipse of an ellipse with the $r^{-3/4}$ temperature distribution of a steady state $\alpha$-model accretion disk. The deeper dashed curve shows the eclipse of an ellipse with a uniform surface brightness on which a bright spot has been superimposed near the outer edge. The spot covers the outer 1/3 of the disk radius, it extends $60°$ around the disk, and it has a surface brightness 4 times greater than the underlying disk. *Lower*: The dashed line is the eclipse of a disk with two bright regions. One is the same outer bright spot as in the upper panel, and the other is a bright region centered on the neutron star and covering the inner 1/3 of the disk.

with two bright regions. One is the same outer bright spot as in the upper panel, and the other is a bright region centered on the neutron star and covering the inner 1/3 of the disk. Once again the eclipse clearly differs from the observed eclipses.

In summary a uniform, elliptical distribution of light with $a_{disk} = 0.3a$ and $e = 0.5$ provides a reasonably good match to the observed eclipse light curves. This model is manifestly incomplete, however. It accounts only for the eclipses, not the other variations in the light curve. At X-ray wavelengths the variations are caused by variable absorption, perhaps by the ADC or vertically extended inner disk, perhaps by a disk rim with a variable height (Hakala et al. 2005). These effects have not been included in the model for the optical eclipse. Nevertheless, the reasonably good fits of the model to the observed eclipses lead us to believe that the model correctly describes the geometry of the optical eclipses.

What can maintain the elliptical brightness distribution and cause it not only to precess but also to maintain a coherent precession period over an entire observing season? It is difficult to understand how a disk with a perfectly circular mass distribution could support such behavior. We hypothesize that the underlying distribution of mass in the disk has a nonaxisymmetric, roughly elliptical component, and that this nonaxisymmetric component is also precessing at the 5.5 day period. Because the 112.6 minute period of the superhump-like modulation is the beat period between the orbital period and the 5.5 day precession period, the superhump-like modulation must be causally related to the precessing disk. In this picture the dynamical behavior of the disk is similar to the dynamical behavior of disks displaying true superhumps. The eccentricity we infer is large but consistent with the largest

eccentricities reached in theoretical calculations of accretion disks (Smith et al. 2007); and it is consistent with the eccentricity deduced for the accretion disk in the cataclysmic variable WZ Sge using techniques similar to ours (Patterson et al. 2002). We reiterate, however, the conclusion of Haswell et al. (2001): The specific mechanism that generates a superhump light curve from a precessing eccentric disk cannot be the same as in the cataclysmic variables.

## 6. DISCUSSION AND CONCLUSION

The main results of this work are as follows:

1. The orbital period of UW CrB is $P_{\rm orb} = 110.976722 \pm 0.000012$ minutes. The eclipse depths vary greatly and can disappear altogether or at least become so shallow that they are hidden by other variability. Even when the eclipses are deep and well defined, the times of mideclipse can deviate by more than $\pm 0.025$ in phase from the best-fit ephemeris.

2. The light curve has a superhump-like modulation with a period $P_{\rm hump} = 112.58 \pm 0.03$ minutes. The modulation is not strictly periodic but does maintain coherence for $\sim 80$ days. The period excess is $\epsilon = (P_{\rm hump} - P_{\rm orb})/P_{\rm orb} \approx 0.0145$, placing UW CrB not far from the empirical $\epsilon(q)$ relation for superhumps in cataclysmic variables and other LMXBs.

3. The morphology of the superhump-like modulation, and the depths and times of eclipse all vary, producing an orbital light curve whose shape changes greatly from night to night. The changes are not random: light-curve shapes recur with a period $P_{\rm recur} = 5.5 \pm 0.1$ days. The three periods are related by the beat relation $P_{\rm orb}^{-1} - P_{\rm recur}^{-1} = P_{\rm hump}^{-1}$.

4. A simple model in which the distribution of light across the accretion disk is elliptical and the elliptical distribution precesses yields light curves that reproduce the eclipse widths, range of eclipse depths, and jitter in the times of mideclipse. The precession period equals the recurrence period, $\sim 5.5$ days. We propose that the underlying distribution of mass in the disk has a nonaxisymmetric, roughly elliptical component, and that this nonaxisymmetric component is also precessing at the 5.5 day period. The dynamical behavior of the disk is, then, similar to the dynamical behavior of disks displaying true superhumps.

5. The eclipse is not consistent with a highly nonuniform distribution of surface brightness across the ellipse. In particular the eclipse is not consistent with distributions that are much brighter near the center of the disk, such as the $r^{-3/4}$ temperature distribution of a steady state, optically thick $\alpha$-model accretion disk.

There is abundant evidence for nonaxisymmetric disks in LMXBs. Doppler tomograms of emission lines from the disks show the ubiquitous presence of streams, arcs, and spots where the emission is enhanced (Hynes et al. 2001; Marsh 2001). X-ray light curves of high-mass X-ray binaries betray the presence of precessing, tilted, twisted accretion disks, most notably in Her X-1, SMC X-1, and LMC X-4 (Clarkson et al. 2003; Leahy 2002; Naik & Paul 2004; Hickox & Vrtilek 2005). We have now shown that the accretion disk in UW CrB has an elliptical distribution of surface brightness, that the elliptical distribution precesses, and that the superhump-like modulation of its light curve is closely related to the elliptical distribution. By implication the superhump-like variations seen in the light curves of other LMXBs are also related to the precession of an elliptical disk—as had already been suspected (O'Donoghue & Charles 1996). The objections raised by Haswell et al. (2001) still hold true, however, so the specific physical mechanism responsible for converting the behavior of the precessing elliptical disk to a superhump-like modulation of the light curve cannot be the same as for the superhumps in cataclysmic variables.

REFERENCES

Clarkson, W. I., Charles, P. A., Coe, M. J., & Laycock, S. 2003, MNRAS, 343, 1213
Ergma, E., & Vilhu, O. 1993, A&A, 277, 483
Foulkes, S. B., Haswell, C. A., & Murray, J. R. 2006, MNRAS, 366, 1399
Frank, J., King, A., & Raine, D. 2002, in Accretion Power in Astrophysics, ed. J. Frank, A. King, & D. Raine (3rd ed.; Cambridge: Cambridge Univ. Press), 141
Gioia, I. M., Maccacaro, T., Schild, R. E., Wolter, A., Stocke, J. T., Morris, S. L., & Henry, J. P. 1990, ApJS, 72, 567
Hakala, P. J., Chaytor, D. H., Vilhu, O., Piirola, V., Morris, S. L., & Muhli, P. 1998, A&A, 333, 540
Hakala, P., Ramsay, G., Muhli, P., Charles, P., Hannikainen, D., Mukai, K., & Vilhu, O. 2005, MNRAS, 356, 1133
Haswell, C. A., King, A. R., Murray, J. R., & Charles, P. A. 2001, MNRAS, 321, 475
Hickox, R. C., & Vrtilek, S. D. 2005, ApJ, 633, 1064
Howell, S. B., Nelson, L. A., & Rappaport, S. 2001, ApJ, 550, 897
Hynes, R. I., Charles, P. A., Haswell, C. A., Casares, J., & Zurita, C. 2001, in Astrotomography: Indirect Imaging Methods in Observational Astronomy, ed. H. M. J. Boffin, D. Steeghs, & J. Cuypers (Berlin: Springer), 378
Hynes, R. I., Robinson, E. L., & Jeffery, E. 2004, ApJ, 608, L101
Jonker, P. G., van der Klis, M., Kouveliotou, C., Méndez, M., Lewin, W. H. G., & Belloni, T. 2003, MNRAS, 346, 684
Leahy, D. A. 2002, MNRAS, 334, 847

Marsh, T. R. 2001, in Astrotomography: Indirect Imaging Methods in Observational Astronomy, ed. H. M. J. Boffin, D. Steeghs, & J. Cuypers (Berlin: Springer), 1
Mineshige, S., Hirose, M., & Osaki, Y. 1992, PASJ, 44, L15
Morris, S. L., Liebert, J., Stocke, J. T., Gioia, I. M., Schild, R. E., & Wolter, A. 1990, ApJ, 365, 686
Muhli, P., Hakala, P. J., Hjalmarsdotter, L., Hannikainen, D. C., & Schultz, J. 2004, Rev. Mex. AA Ser. Conf., 20, 211
Mukai, K., Smale, A. P., Stahle, C. K., Schlegel, E. M., & Wijnands, R. 2001, ApJ, 561, 938
Murray, J. R. 2000, MNRAS, 314, L1
Naik, S., & Paul, B. 2004, ApJ, 600, 351
O'Donoghue, D., & Charles, P. A. 1996, MNRAS, 282, 191
Patterson, J. 2001, PASP, 113, 736
Patterson, J., et al. 2002, PASP, 114, 721
Pearson, K. J. 2006, MNRAS, 371, 235
Smith, A. J., Haswell, C. A., Murray, J. R., Truss, M. R., & Foulkes, S. B. 2007, MNRAS, 378, 785
Stellingwerf, R. F. 1978, ApJ, 224, 953
Thorsett, S. E., & Chakrabarty, D. 1999, ApJ, 512, 288
Vilhu, O., Hakala, P., & Ergma, E. 1993, in Cataclysmic Variables and Related Physics, ed. O. Regev & G. Shaviv (Bristol: IOP), 73
Warner, B. 1995, Cataclysmic Variable Stars (Cambridge: Cambridge Univ. Press)